Volume 183, number 2 FEBS 2453 April 1985

Selective oxidative destruction of iron-sulfur clusters

Ferricyanide oxidation of *Azotobacter vinelandii* ferredoxin I

T.V. Morgan°, P.J. Stephens+, F. Devlin, B.K. Burgess* and C.D. Stout†

*Department of Chemistry, University of Southern California, Los Angeles, CA 90089-0482, *Department of Molecular Biology and Biochemistry, University of California at Irvine, Irvine, CA 92717,* and †*Department of Crystallography, University of Pittsburgh, Pittsburgh, PA 15260, USA*

Received 30 Janaury 1985

The destructive oxidation of aerobically isolated 7Fe *Azotobacter vinelandii* ferredoxin I [(7Fe)FdI] by $Fe(CN)_6^{3-}$ is examined using low-temperature magnetic circular dichroism (MCD) and EPR. The results demonstrate that oxidation of the [3Fe-3S] cluster occurs only after essentially complete destruction of the [4Fe-4S] cluster. It is therefore feasible by controlled $Fe(CN)_6^{3-}$ oxidation to obtain a partially metallated form of FdI, (3Fe)FdI, containing only a [3Fe-3S) cluster. The MCD and EPR data demonstrate that the [3Fe-3S] cluster in (3Fe)FdI is essentially identical in structure to that in the native protein.

Iron-sulfur cluster *Ferredoxin I* *Oxidative destruction* A. vinelandii

1. INTRODUCTION

X-ray crystallography [1,2] and Mossbauer spectroscopy [3] have recently shown that *Azotobacter vinelandii* ferredoxin I [(7Fe)FdI], isolated aerobically, possesses two iron-sulfur (Fe-S) clusters, containing respectively 3 and 4 Fe. (We use the designation (7Fe)FdI, since we have recently shown that ferredoxin I can be reconstituted as an 8Fe, $\{2[4Fe\text{-}4S]^{1+/2+}\}$ protein: (8Fe)FdI [4].) The [3Fe-3S] cluster [1,2] in (7Fe)FdI as isolated is paramagnetic [3], and thus responsible for the near-isotropic $g \sim 2.01$ EPR [5], and is reduced by dithionite [3]. The [4Fe-4S] cluster is diamagnetic in (7Fe)FdI as isolated [3], reacts with $Fe(CN)_6^{3-}$ generating EPR at $g \sim 2.0$ [5] and was reported to be not reducible [5]. This behavior led originally to identification of the [4Fe-4S] cluster as a HIPIP-type, $[4Fe\text{-}4S]^{2+/3+}$ cluster [5]. However, we have recently shown [6,7] that (i) the product of the reaction with $Fe(CN)_6^{3-}$ is not a HIPIP-type cluster and (ii) that at pH $\gtrsim$ 8 a reduced, $[4Fe\text{-}4S]^{1+}$ cluster EPR can be generated by dithionite; the [4Fe-4S] cluster is thus a low-potential, $[4Fe\text{-}4S]^{1+/2+}$ cluster of the type observed in bacterial ferredoxins.

Our studies of the $Fe(CN)_6^{3-}$ oxidation of isolated (7Fe)FdI, $(7Fe)FdI_{ox}$, showed that the reaction is progressive and destructive of the Fe-S clusters [6]. At a $[Fe(CN)_6^{3-}]:[(7Fe)FdI_{ox}]$ ratio $\gtrsim$ 25, UV-visible absorption and circular dichroism (CD) and EPR attributable to Fe-S clusters are eliminated. Initial reaction leads to production of additional $g \gtrsim 2.0$ EPR intensity, which is maximised by $[Fe(CN)_6^{3-}]:[(7Fe)FdI_{ox}] \sim 3$. The EPR-active species created possesses unusual EPR and magnetic circular dichroism (MCD) characteristics; notably, its liquid helium temperature visible-near-UV paramagnetic MCD is so weak as to be not observable (in the presence of the paramagnetic [3Fe-3S] cluster). We therefore proposed that the initial $Fe(CN)_6^{3-}$ reaction involves oxidation of S-containing moieties of the $[4Fe\text{-}4S]^{2+}$ cluster in which a radical (specifically, a cysteinyldisulfide radical) is formed.

+ To whom correspondence should be addressed
° Present address: Exxon Research and Engineering Co., Annandale, NJ 08801, USA

Published by Elsevier Science Publishers B.V. (Biomedical Division)
00145793/85/$3.30

We now report further studies of the $Fe(CN)_6^{3-}$ oxidation of (7Fe)FdI_{ox} by MCD and EPR which show that at $[Fe(CN)_6^{3-}]:[(7Fe)FdI_{ox}] > 3$ the oxidation of the [4Fe-4S] cluster continues to occur preferentially, and that oxidation of the [3Fe-3S] cluster is only initiated following nearly complete [4Fe-4S] cluster destruction. While selective, reversible oxidation of different Fe-S clusters in proteins is well known, selective destructive oxidation is not. The latter is unlikely to be of physiological significance, of course. However, as a route to preparation of partially metallated proteins it is of considerable interest. In the case of (7Fe)FdI, this work shows that it is feasible to prepare a 3Fe form of FdI from which the [4Fe-4S] cluster has been removed and containing only the [3Fe-3S] cluster. This in turn will allow the physical and chemical properties of the [3Fe-3S] cluster to be explored in the absence of background from the [4Fe-4S] cluster, a prospect of particular value in view of current controversy over the uniformity of 3Fe cluster structures [8].

2. MATERIALS AND METHODS

All materials and methods were as in earlier work [4,6]. Samples of $Fe(CN)_6^{3-}$-oxidised (7Fe)FdI_{ox} for MCD were prepared by incubation of (7Fe)FdI_{ox} with $Fe(CN)_6^{3-}$ until the absorption and CD became constant (the time for equilibration increases with $[Fe(CN)_6^{3-}]:[(7Fe)FdI_{ox}]$, being ~2 h at a ratio of ~20 at the concentration and temperatures employed). Glycerol was added to ~50:50 (v/v). The protein concentration change on addition of glycerol was obtained by absorption and CD, which also confirmed the absence of any perturbation of the protein structure by glycerol. The MCD cell path length was measured prior to freezing using a micrometer. Samples of $Fe(CN)_6^{3-}$-oxidised (7Fe)FdI_{ox} for EPR were incubated uniformly for 2 h prior to freezing. EPR tubes were calibrated using the room-temperature EPR of 4-hydroxy-2,2,6,6-tetramethylpiperidinyloxyl free radical. EPR intensities were integrated [9] using 1 mM CuEDTA as a standard. All experiments, subsequent to purification of (7Fe)FdI_{ox}, were anaerobic. 0.1 M potassium phosphate buffer, pH 7.5, was used throughout.

3. RESULTS AND DISCUSSION

The visible-near-UV MCD of $Fe(CN)_6^{3-}$-oxidised (7Fe)FdI_{ox} at $[Fe(CN)_6^{3-}]:[(7Fe)FdI_{ox}]$ ratios from 0 to ~20 was measured at ~2 K and ~3 tesla. Below 4 K the MCD of (7Fe)FdI_{ox} is attributable entirely to the $S = 1/2$ ground electronic state of the oxidised, $[3Fe\text{-}3S]^{3+}$ cluster (the assignment of a 3+ charge to the oxidised [3Fe-3S] cluster follows from the Fe^{3+} oxidation level of all 3Fe [10], together with the Fe_3S_3 core stoichiometry) [5,11]. After oxidation by $Fe(CN)_6^{3-}$, the ~2 K MCD exhibits the following features: (i) within experimental error, no change in shape occurs; (ii) only at $[Fe(CN)_6^{3-}]:[(7Fe)FdI_{ox}] \gtrsim 10$ does the MCD intensity diminish. These results are illustrated in figs 1 and 2. Fig.1 shows the MCD at $[Fe(CN)_6^{3-}]:[(7Fe)FdI_{ox}] = 0$, 8.5, 13.3 and 20.1, normalized to constant amplitude of difference from 344 nm to 383 nm. This makes clear the constancy in shape of MCD over the entire range of $[Fe(CN)_6^{3-}]:[(7Fe)FdI_{ox}]$ ratios. Fig.2 plots the variation in absolute MCD intensity, normalized with respect to concentration (c), pathlength (l) and temperature variation using the expression [11]: $\Delta A = (\Delta\epsilon)_0 cl \tanh(2.01\beta H/2kT)$ (where H is the magnetic field and T is the absolute temperature). This complex expression is required since at ~2 K, magnetic fields of ~3 tesla cause appreciable saturation of the MCD.

From the invariance of MCD shape to $Fe(CN)_6^{3-}$ oxidation it follows that (i) at all $[Fe(CN)_6^{3-}]:[(7Fe)FdI_{ox}]$ ratios studied, no unreduced $Fe(CN)_6^{3-}$ remains, since $Fe(CN)_6^{3-}$ possesses extremely large paramagnetic MCD; and (ii) no oxidation products, whether bound to the protein or not, exhibit significant paramagnetic MCD in the spectral range studied. As a consequence it follows that (i) the concentration of intact $[3Fe\text{-}3S]^{3+}$ cluster is directly proportional to the magnitude of the MCD signal and (ii) there is no evidence of change in the structure of the $[3Fe\text{-}3S]^{3+}$ cluster during oxidation of the [4Fe-4S] cluster, since the shape of its spectrum does not measurably alter.

The EPR of $Fe(CN)_6^{3-}$-oxidised (7Fe)FdI_{ox} at $[Fe(CN)_6^{3-}]:[(7Fe)FdI_{ox}]$ ratios from 0 to 30 has been measured at 11 and 50 K. At 11 K (7Fe)FdI_{ox} exhibits a sharp, nearly isotropic EPR spectrum with $g \sim 2.01$; at 50 K this signal is broadened to undetectability [6]. On oxidation with $Fe(CN)_6^{3-}$,

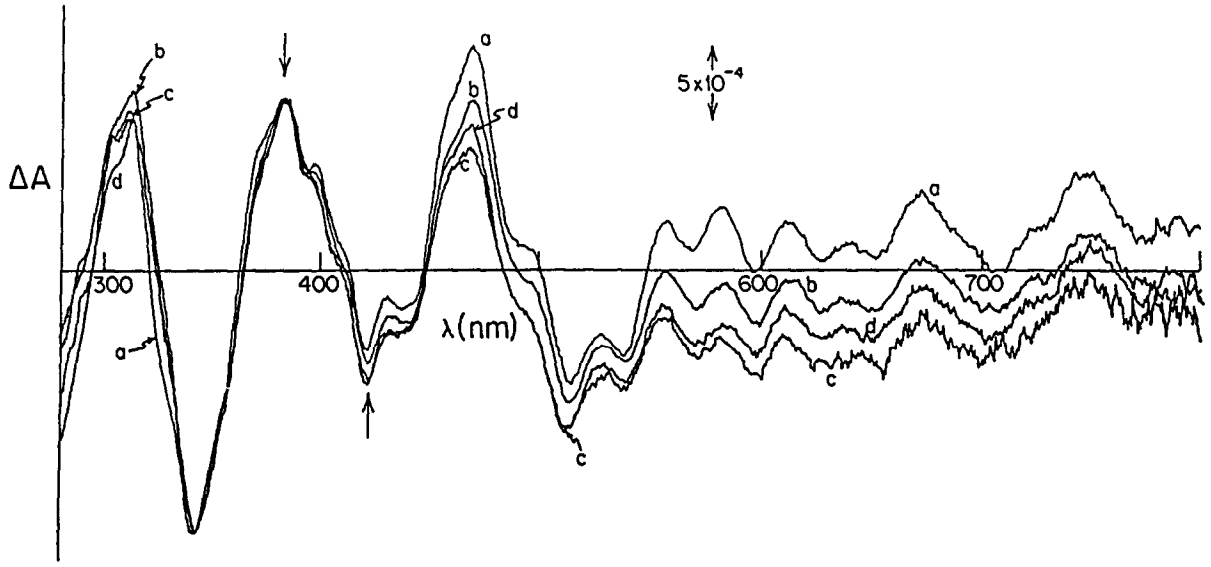

Fig.1. MCD of $Fe(CN)_6^{3-}$-oxidised (7Fe)FdI_{ox} at ~2 K and ~3 tesla. $[Fe(CN)_6^{3-}]$:[(7Fe)FdI_{ox}] was: (a) 0, (b) 8.5, (c) 13.3, (d) 20.1. In curve a, (7Fe)FdI_{ox} is 0.163 mM in 0.1 M potassium phosphate buffer, pH 7.5, prior to addition of glycerol, and 0.081 mM after addition of glycerol. In b–d, the MCD is plotted after normalization to curve a, using the MCD difference between 344 and 383 nM (indicated by arrows). In all experiments, [(7Fe)FdI] was in the range 0.072–0.094 mM (after addition of glycerol), the temperature was 1.78 K and the magnetic field was 2.81 tesla.

the 11 K EPR first broadens, then diminishes in amplitude, as shown in fig.3. At 50 K, an anisotropic signal appears, whose amplitude first increases and then decreases, the shape remaining constant throughout [6]. (The 50 K EPR spectra shown in [6] were obtained after ~1 h incubation of (7Fe)FdI_{ox} and $Fe(CN)_6^{3-}$. At $[Fe(CN)_6^{3-}]$:[(7Fe)FdI_{ox}] $\gtrsim$ 10, equilibration is incomplete in 1 h and the spectra in [6] exhibit greater EPR intensity than in the fully equilibrated samples used here.) The maximum integrated intensities of the EPR at 11 and 50 K, which occur at $[Fe(CN)_6^{3-}]$:[(7Fe)FdI_{ox}] close to 3, are 1.7 and 0.8 spin/molecule, respectively. The intensity of the 50 K signal is plotted in fig.2.

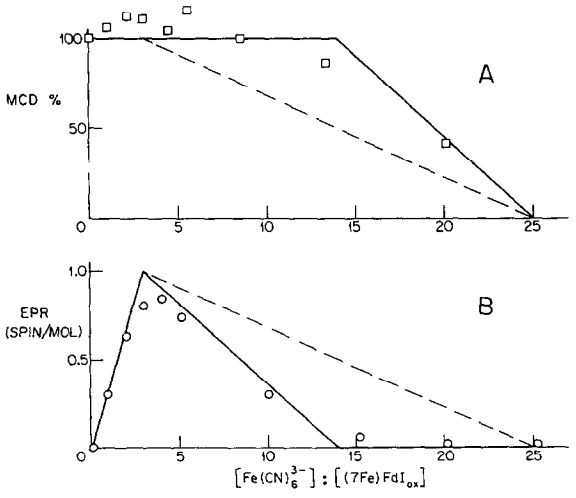

Fig.2. (A) Relative MCD intensities of $Fe(CN)_6^{3-}$-oxidised (7Fe)FdI_{ox}. In all experiments, [(7Fe)FdI_{ox}] was 0.063–0.094 mM (after addition of glycerol). Temperatures were in the range 1.77–2.00 K and the magnetic field was 2.81 tesla. The relative intensities plotted are the averages of the differences in MCD between 313 and 343 nm, 344 and 383 nm, 383 and 422 nm, 422 and 470 nm, and 470 and 515 nm. The MCD at each $[Fe(CN)_6^{3-}]$:[(7Fe)FdI_{ox}] was normalised to the MCD of (7Fe)FdI_{ox} using $\Delta A = (\Delta\epsilon)_0 cl \tanh(2.01\beta H/2kT)$ [see text]. (B) EPR intensities of $Fe(CN)_6^{3-}$-oxidised (7Fe)FdI_{ox} at 50 K. The intensity at $[Fe(CN)_6^{3-}]$:[(7Fe)FdI_{ox}] = 3.1 is obtained by integration. At all other $[Fe(CN)_6^{3-}]$:[(7Fe)FdI_{ox}] ratios, the relative peak-to-peak amplitudes from $g = 2.01$ to $g = 1.98$ were measured and scaled to the intensity at the ratio of 3.1. The dashed lines are the prediction of scheme 1; the solid lines are predicted by scheme 2.

As discussed previously [6], the initial oxidation of (7Fe)FdI$_{ox}$ involves 3-electron oxidation of the [4Fe-4S]$^{2+}$ cluster to a species (labelled [4Fe-4S]′) responsible for the 50 K EPR signal:

$$\{[3Fe\text{-}3S]^{3+},[4Fe\text{-}4S]^{2+}\} \longrightarrow \{[3Fe\text{-}3S]^{3+},[4Fe\text{-}4S]'\}$$

(7Fe)FdI$_{ox}$ (7Fe)FdI$'_{ox}$

Two simple possibilities exist for the further oxidation:

$$\{[3Fe\text{-}3S]^{3+},[4Fe\text{-}4S]'\} \longrightarrow \{-,-\} \quad (1)$$

$$(7Fe)FdI'_{ox} \longrightarrow \text{apo-FdI}$$

or

$$\{[3Fe\text{-}3S]^{3+},[4Fe\text{-}4S]'\} \longrightarrow \{[3Fe\text{-}3S]^{3+},-\} \longrightarrow \{-,-\} \quad (2)$$

$$(7Fe)FdI'_{ox} \longrightarrow (3Fe)FdI_{ox} \longrightarrow \text{apoFdI}$$

where – indicates absence of Fe-S cluster. In reaction 1, [3Fe-3S]$^{3+}$ and [4Fe-4S]′ are destroyed simultaneously and no intermediate, partially metallated species exist. In reaction 2, destruction of [4Fe-4S]′ proceeds preferentially, leading to an intermediate, (3Fe)FdI$_{ox}$, containing only a [3Fe-3S]$^{3+}$ cluster, which is subsequently oxidised. The MCD and EPR intensities predicted by sequences 1 and 2 differ, as shown in fig.2. We assume [6], following Petering et al. [12], that the terminal oxidation states of the Fe-S cluster constituents are Fe^{3+}, S^0 and cys-$S^{\cdot}$. The [3Fe-3S]$^{3+}$ and [4Fe-4S]$^{2+}$ clusters then require removal of 11 and 14 electrons, respectively, for complete destruction on the basis of stoichiometries of [Fe_3S_3(S-cys)$_5$] and [Fe_4S_4(S-cys)$_4$], respectively.

As fig.2 shows, the experimental data are close to the expectations of sequence 2 and far from those of sequence 1. The differences from the theoretical behavior for sequence 2 can be attributed either to overlapping of subsequent reaction stages (destruction of the [3Fe-3S]$^{3+}$ cluster

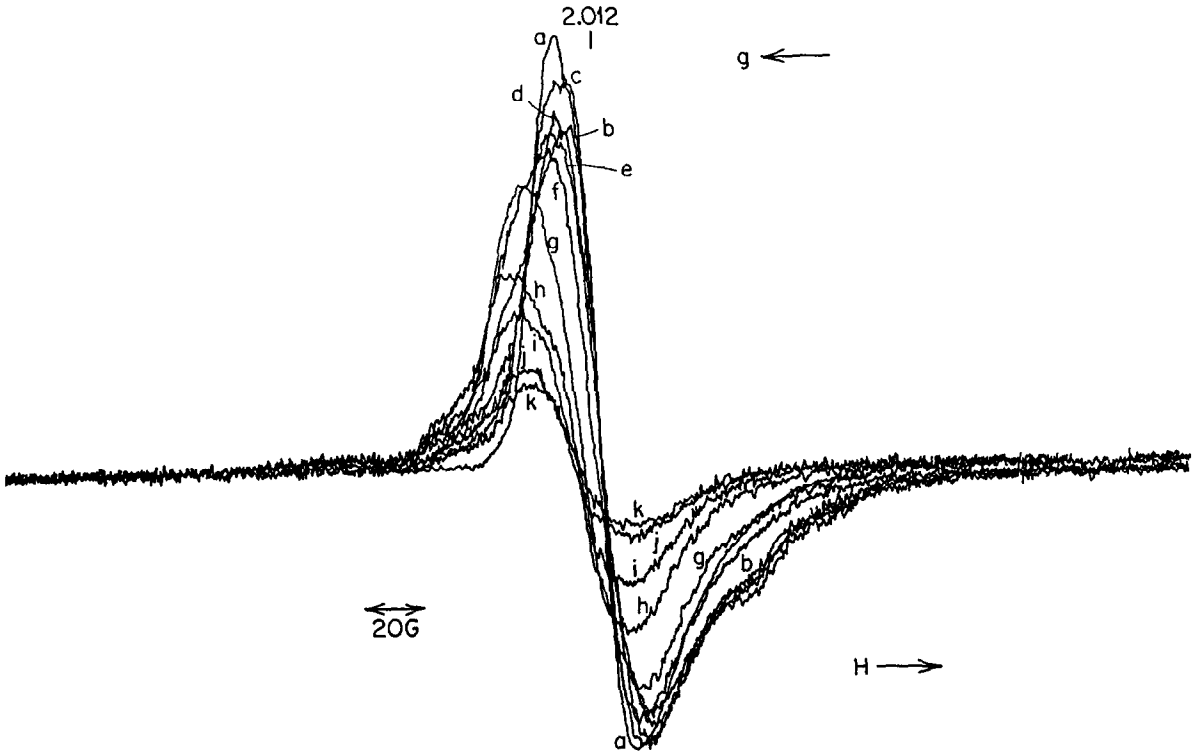

Fig.3. EPR of $Fe(CN)_6^{3-}$-oxidised (7Fe)FdI$_{ox}$ at 11 K. [$Fe(CN)_6^{3-}$]:[(7Fe)FdI$_{ox}$] was: (a) 0, (b) 1.0, (c) 2.1, (d) 3.1, (e) 4.0, (f) 5.1, (g) 10.1, (h) 15.2, (i) 20.2, (j) 25.3, (k) 30.5. (7Fe)FdI$_{ox}$ was 0.041 mM in 0.1 M potassium phosphate buffer, pH 7.5, after addition of $Fe(CN)_6^{3-}$ throughout. Incubation time was 2 h. Power, frequency, modulation and gain were 2 mW, 9.354 GHz, 1 G and 2.5×10^4, respectively. EPR tube sizes varied ~15%.

beginning prior to complete destruction of $[4Fe\text{-}4S]^{2+}$ cluster) or to uncertainties in experimental MCD and EPR intensities (or both).

It follows that in the terminal phase of $Fe(CN)_6^{3-}$ oxidation of (7Fe)FdI_{ox}, only two species are present: (3Fe)FdI_{ox} and apo-FdI. Oxidation to this level followed by separation of metalloprotein from apoprotein should then yield homogeneous (3Fe)FdI_{ox}. Further, the MCD and EPR data show that the $[3Fe\text{-}3S]^{3+}$ cluster of (3Fe)FdI_{ox} is very little altered by destruction of the $[4Fe\text{-}4S]^{2+}$ cluster. The MCD shows no significant change; the 11 K EPR is slightly broader than (7Fe)FdI_{ox}. The physical and chemical properties of the $[3Fe\text{-}3S]^{3+}$ cluster of (3Fe)FdI_{ox} should then be directly relevant to those of the $[3Fe\text{-}3S]^{3+}$ cluster in (7Fe)FdI_{ox}. It should be added, however, that at this time we have no information regarding the disposition of the products of oxidation of the S^{2-} and cysteine initially involved in the $[4Fe\text{-}4S]^{2+}$ cluster. It is possible that cysteine di- and/or trisulfide linkages are formed, either intra- or intermolecularly or both. (3Fe)FdI could therefore be of higher M_r than (7Fe)FdI. We are currently pursuing the purification and characterisation of (3Fe)FdI.

ACKNOWLEDGEMENTS

This work was supported by the National Institutes of Health and the National Science Foundation.

REFERENCES

[1] Ghosh, D., Furey, W., O'Donnell, S. and Stout, C.D. (1981) J. Biol. Chem. 256, 4185–4192.
[2] Ghosh, D., O'Donnell, S., Furey, W., Robbins, A.H. and Stout, C.D. (1982) J. Mol. Biol. 158, 73–109.
[3] Emptage, M.H., Kent, T.A., Huynh, B.H., Rawlings, J., Orme-Johnson, W.H. and Munck, E. (1980) J. Biol. Chem. 255, 1793–1796.
[4] Morgan, T.V., Stephens, P.J., Burgess, B.K. and Stout, C.D. (1984) FEBS Lett. 167, 137–141.
[5] Sweeney, W.V., Rabinowitz, J.C. and Yoch, D.C. (1975) J. Biol. Chem. 250, 7842–7847.
[6] Morgan, T.V., Stephens, P.J., Devlin, F., Stout, C.D., Melis, K.A. and Burgess, B.K. (1984) Proc. Natl. Acad. Sci. USA 81, 1931–1935.
[7] Morgan, T.V., Stephens, P.J., Stout, C.D. and Burgess, B.K. FEBS Lett., submitted.
[8] Beinert, H. and Thomson, A.J. (1983) Arch. Biochem. Biophys. 222, 333–361.
[9] Wyard, S.J. (1965) J. Sci. Instrum. 42, 769–770.
[10] Kent, T.A., Huynh, B.H. and Munck, E. (1980) Proc. Natl. Acad. Sci. USA 77, 6574.
[11] Stephens, P.J., Morgan, T.V., Devlin, F., Stout, C.D., Burgess, B.K., Ellis, W.R., Gray, H.B., Beinert, H. and Emptage, M.H. (1985) Biochemistry, submitted.
[12] Petering, D., Fee, J.A. and Palmer, G. (1971) J. Biol. Chem. 246, 643–653.